

# Depletion of CLL cells by venetoclax treatment reverses oxidative stress and impaired glycolysis in CD4 T cells

J. A. C. van Bruggen,<sup>1-3</sup> G. J. W. van der Windt,<sup>1-3</sup> M. Hoogendoorn,<sup>4</sup> J. Dubois,<sup>1-3</sup> Arnon P. Kater,<sup>1-3</sup> and F. S. Peters<sup>1-3</sup>

<sup>1</sup>Department of Hematology, Cancer Center Amsterdam, <sup>2</sup>Lymphoma and Myeloma Center Amsterdam, and <sup>3</sup>Department of Experimental Immunology, Amsterdam Infection & Immunity Institute, University of Amsterdam, Amsterdam University Medical Center, Amsterdam, The Netherlands; and <sup>4</sup>Department of Internal Medicine, Medical Center Leeuwarden, Leeuwarden, The Netherlands

## Key Points

- CLL-derived CD4<sup>+</sup> T cells have an abnormal redox balance, and glycolytic switch is impaired, which is restored upon elimination of CLL cells.
- CLL elimination in vivo by venetoclax plus obinutuzumab treatment restores T-cell activation and proliferation.

Acquired T-cell dysfunction is characteristic of chronic lymphocytic leukemia (CLL) and is associated with reduced efficacy of T cell–based therapies. A recently described feature of dysfunctional CLL-derived CD8 T cells is reduced metabolic plasticity. To what extent CD4 T cells are affected and whether CD4 T-cell metabolism and function can be restored upon clinical depletion of CLL cells are currently unknown. We address these unresolved issues by comprehensive phenotypic, metabolic, transcriptomic, and functional analysis of CD4 T cells of untreated patients with CLL and by analysis of the effects of venetoclax plus obinutuzumab on the CD4 population. Resting CD4 T cells derived from patients with CLL expressed lower levels of GLUT-1 and displayed deteriorated oxidative phosphorylation (OXPHOS) and overall reduced mitochondrial fitness. Upon T-cell stimulation, CLL T cells were unable to initiate glycolysis. Transcriptome analysis revealed that depletion of CLL cells in vitro resulted in upregulation of OXPHOS and glycolysis pathways and restored T-cell function in vitro. Analysis of CD4 T cells from patients with CLL before and after venetoclax plus obinutuzumab treatment, which led to effective clearance of CLL in blood and bone marrow, revealed recovery of T-cell activation and restoration of the switch to glycolysis, as well as improved T-cell proliferation. Collectively, these data demonstrate that CLL cells impose metabolic restrictions on CD4 T cells, which leads to reduced CD4 T-cell functionality. This trial was registered in the Netherlands Trial Registry as #NTR6043.

## Introduction

Acquired failure of the immune system is a common occurrence in patients with chronic lymphocytic leukemia (CLL).<sup>1,2</sup> Current literature suggests that interaction between CLL and T cells pushes CD8<sup>+</sup> T cells toward a dysfunctional phenotype, as indicated by increased expression of inhibitory molecules CD244, CD160, and programmed death-1 (PD-1),<sup>3-6</sup> failure of T-cell proliferation,<sup>5,7</sup> and impaired formation of the immunologic synapse.<sup>8</sup> T-cell function and metabolism are tightly connected. Resting T cells primarily use oxidative phosphorylation (OXPHOS) to support the energy requirements.<sup>9</sup> Upon activation, T cells increase OXPHOS but even more dramatically enhance glycolysis activity, which then becomes the dominant metabolic pathway. This switch to an anabolic metabolism is required to provide the cells with a source of biomass that is essential for effector functions and proliferation.<sup>9,10</sup> We have shown that CD8 T cells in CLL have impaired glucose metabolism upon activation and decreased mitochondrial

Submitted 24 January 2022; accepted 10 May 2022; prepublished online on *Blood Advances* First Edition 17 May 2022; final version published online 19 July 2022. DOI 10.1182/bloodadvances.2022007034.

Sequencing data can be found in the Gene Expression Omnibus at [ncbi.nlm.nih.gov/geo](https://ncbi.nlm.nih.gov/geo) (accession #GSE19367). Contact the corresponding author for other forms of data sharing at [a.p.kater@amsterdamumc.nl](mailto:a.p.kater@amsterdamumc.nl).

The full-text version of this article contains a data supplement.

© 2022 by The American Society of Hematology. Licensed under Creative Commons Attribution-NonCommercial-NoDerivatives 4.0 International (CC BY-NC-ND 4.0), permitting only noncommercial, nonderivative use with attribution. All other rights reserved.

fitness in the resting state,<sup>7,11</sup> both of which could contribute to the low efficacy of T cell–based therapies in CLL.<sup>12</sup> Although a clear relation between metabolism and function was recently described in CD8 T cells of patients with CLL,<sup>7</sup> CD4 T-cell metabolism remains an unexplored but important issue to address, because these cell types can play distinct roles in CLL.

The role of CD4 T cells in CLL is ambiguous,<sup>13</sup> because CD4 subsets potentially have a tumor supportive role in CLL. T helper cells can provide survival signals to CLL cells in the lymph node environment, and regulatory T cells (Tregs) mediate immune tolerance and are found in higher frequency in patients with CLL.<sup>13–15</sup> Upon treatment with Bruton tyrosine kinase inhibitor ibrutinib and BCL-2 inhibitor venetoclax in patients with CLL, numbers of Tregs are reduced and immune cell recovery is observed.<sup>15–18</sup> Effects of targeted CLL depletion by venetoclax-based treatment on the CD4 compartment are currently unknown. We address these unresolved issues by a comprehensive phenotypic, metabolic, transcriptomic, and functional analysis of CD4 lymphocytes of untreated patients with CLL and by analysis of the effects of CLL depletion by a venetoclax-based treatment regimen on the CD4 population.

CD4 T cells had impaired glucose and mitochondrial metabolism, which was restored upon removal of CLL cells. We also reveal that in vivo depletion of CLL with 12 cycles of venetoclax with addition of obinutuzumab (a glycoengineered humanized type 2 anti-CD20 monoclonal antibody inducing strong antibody-dependent cytotoxicity<sup>19</sup>) during the first 6 cycles<sup>20</sup> restored CD4 T-cell function; CD4 T cells were efficiently activated and were able to switch to glycolysis after T-cell stimulation, and T-cell proliferation was also improved. These data indicate that CLL cells impose metabolic restrictions on CD4 T cells and that venetoclax plus obinutuzumab restores T-cell function and metabolism by eliminating leukemic cells.

## Methods

### Patient and HD materials

Peripheral blood was obtained from patients with CLL and age-matched healthy donors (HDs) after written informed consent. Peripheral blood mononuclear cells (PBMCs) from patients with CLL (supplemental Table 1) and age-matched HDs (supplemental Table 2) were obtained and cryopreserved as previously described.<sup>7,21</sup> All HDs were age  $\geq 60$  years and were phenotypically assessed to exclude cases with monoclonal B-cell lymphocytosis. In addition, PBMCs were collected from patients with CLL enrolled in the phase 2 HOVON 139/GIVE trial (supplemental Table 3) at baseline and after 14 treatment cycles. The treatment regimen consisted of preinduction with 2 cycles of obinutuzumab monotherapy (1000 mg daily after dose escalation), induction with combined venetoclax (ramp-up to 400 mg) and obinutuzumab (1000 mg; cycles 3–8), and venetoclax monotherapy (400 mg; cycles 9–14). The study was approved by the Medical Ethical Committee of the Academic Medical Center of Amsterdam and conducted according to the principles of the Declaration of Helsinki.

### Flow cytometry and cell culture

Cryopreserved PBMCs were thawed and adjusted to a concentration of  $3 \times 10^6$  cells per mL and cultured in RPMI 1640 medium (Gibco) supplemented with 10% fetal calf serum, penicillin, and streptomycin (15140-122; Thermo Fischer Scientific) at 37°C with 5% carbon

dioxide. T cells were stimulated using soluble CD3 (clone 1XE; Sanquin) and CD28 (clone 15E8; Sanquin) for up to 10 days. Proliferation was determined by using 123count eBeads (01-1234-42; Thermo Fischer Scientific) according to manufacturer instructions or CellTrace Violet (C34557; Thermo Fischer Scientific). PBMCs were stained as described previously.<sup>7</sup> The following antibodies were used for flow cytometry: CD3 (56-0038-82; eBioscience), CD4 (555349; BD Biosciences and 317442; BioLegend), CD8 (580347 and 563823; BD Biosciences), CD25 (340907 and 563701; BD Biosciences), CD27 (563816; BD Biosciences), CD45RA (563953; BD Biosciences and 304135; BioLegend), CD71 (563768; BD Biosciences and 11-0719-41; eBioscience), PD-1 (561272; BD Biosciences), and GLUT-1 (Glut1-G100; Metafora Biosystems). The following dyes were used to measure metabolic parameters in live T cells (all from Thermo Fischer Scientific): MitoSOX (M36008), MitoTracker Orange (M7510), MitoTracker Green (M7514), and 2-NBDG (N13195). Cells were incubated with metabolic dyes in Hanks balanced salt solution for 15 minutes at 37°C at a final concentration of  $3 \times 10^6$  cells per mL. To measure intracellular proteins PGC1 $\alpha$  (ab77210; Abcam), SOD2 (13141S; Cell Signaling), NFR-2 (ab194984; Abcam), and HO-1 (ADI-OSA-111PE-F; Enzo LifeSciences), T cells were fixed using a fixation and permeabilization kit (554714; BD Biosciences). T cells were measured on an LSR Fortessa (BD Biosciences) and analyzed using FlowJo (version 10.7.1).

### Extracellular flux analysis

Seahorse XF96 or XFp extracellular flux analyzers (Agilent) were used to analyze isolated CD4<sup>+</sup> T cells as previously described.<sup>7,22</sup> Spare respiratory capacity (SRC) was calculated as the ratio between maximum and basal oxygen consumption rates (OCRs). Results were analyzed using Seahorse Wave (version 2.4).

### RNA sequencing

For RNA sequencing, CLL PBMCs were activated with  $\alpha$ CD3/ $\alpha$ CD28 in the original PBMC pool or after T-cell enrichment using a negative T-cell selection kit following manufacturer protocol (17951; StemCell); after 48 hours, viable CD4 T cells were sorted from both conditions using fluorescence-activated cell sorting on the SH800 Cell Sorter (Sony). Cells were pelleted and lysed, and total RNA was isolated using the RNeasy Micro Kit (Qiagen) according to the manufacturer protocol. RNA quality was assessed using a fragment analyzer, and libraries were generated using the NEBNext Ultra II Directional RNA Library Prep Kit for Illumina. Samples were barcoded and sequenced using a NovaSeq6000 (paired-end sequencing at 150 bp per read). Quality of the sequencing data was assessed using FastQC. Raw FastQ files were aligned to the GRCh38 human genome using STAR (version 2.7.9a),<sup>23</sup> and the .transcriptome.out-bam files were used as input for RSEM-calculate-expression (version 1.3.3) to generate expected counts.<sup>24</sup> Normalized counts were generated with DESeq2<sup>25</sup> and plotted with the gplots heatmap.2 function; significant differential expression was determined at false-discovery rate  $< 0.05$ . Gene set enrichment analysis (GSEA) was performed on a matrix of normalized counts using the GSEA desktop application (version 4.1.0). Our data were compared against Hallmark Signatures (h.all.v7.4) gene sets using 1000 permutations.

### Data presentation and statistical analysis

Error bars are shown as standard errors of the mean. All data were tested for normality using a D'Agostino-Pearson omnibus test.

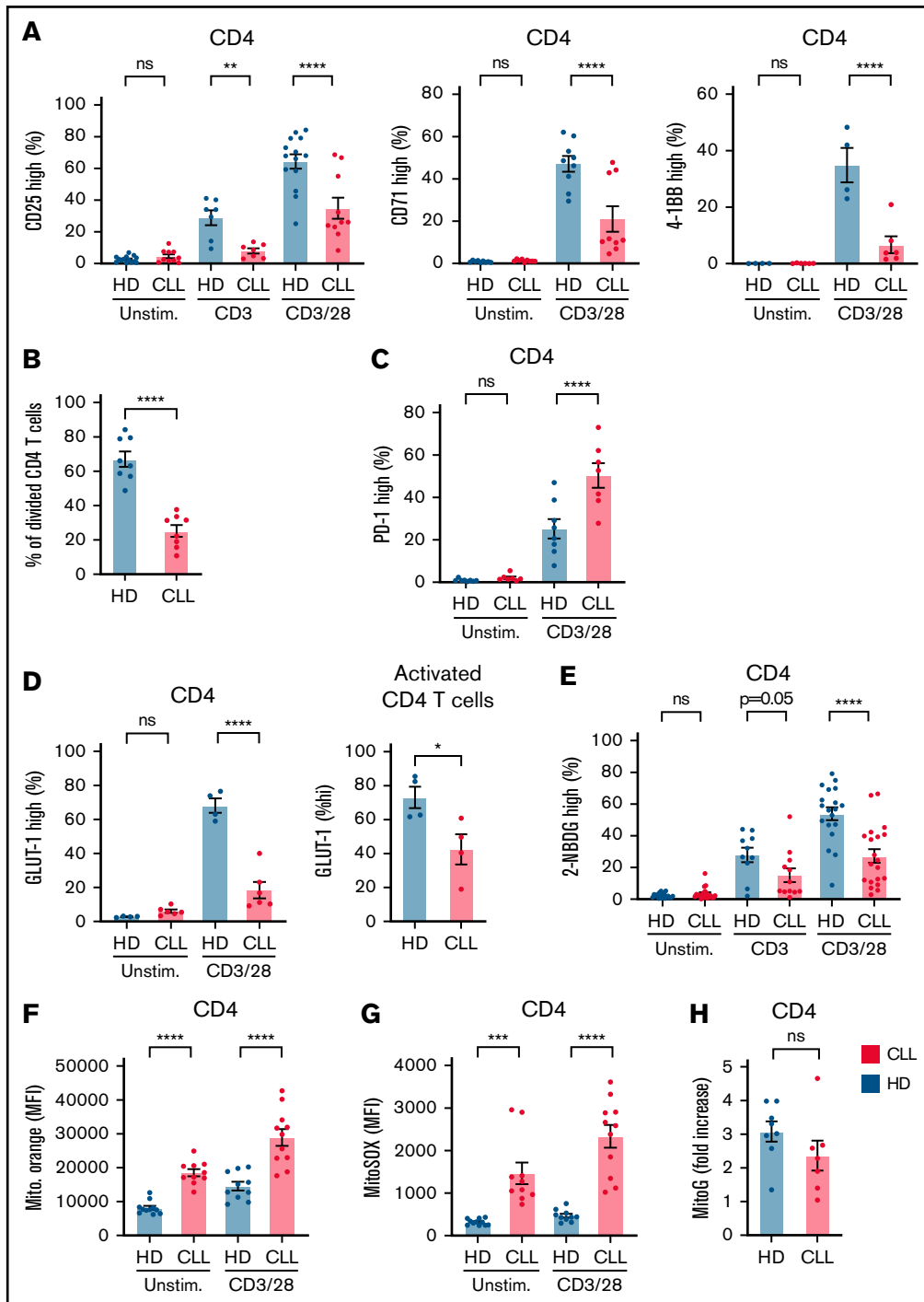


**Figure 1. Impaired glycolytic switch in CLL-derived CD4 T cells.** PBMCs from patients with CLL and HDs were thawed, and T cells were stimulated for 2 or 5 days using either CD3, or CD3 plus CD28 antibodies. Subsequently, CD4 T cells were analyzed by flow cytometry for CD25, CD71, and 4-1BB expression after 2 days (A). Proliferation (B) and PD-1 expression (C) of CD4 T cells were analyzed after 5 days of CD3 plus CD28 stimulation using CellTrace Violet. (D) Glucose transporter GLUT-1 was measured on resting and activated T cells derived from patients with CLL and HDs after 2 days of CD4 T-cell activation. GLUT-1 expression was measured on activated (CD25<sup>+</sup>) T cells (right). (E) Glucose uptake (2-NBDG) was measured in activated CD4 T cells after stimulation using CD3 or CD3 plus CD28 antibodies for 2 days. Mitochondrial membrane potential (MitoTracker Orange) (F) and mitochondrial reactive oxygen species (ROS; MitoSOX) (G) was measured in T cells activated for 2 days with CD3 plus CD28 antibodies. (H) Mitochondrial biogenesis (calculated as ratio of MitoTracker Green mean fluorescence intensity (MFI) in T cells 2 days after activation over unstimulated T cells). Each dot represents a different HD or patient with CLL. Data are presented as mean  $\pm$  standard error of the mean. \* $P < .05$ , \*\* $P < .005$ , \*\*\* $P < .001$ , \*\*\*\* $P < .0001$ . ns, not significant.

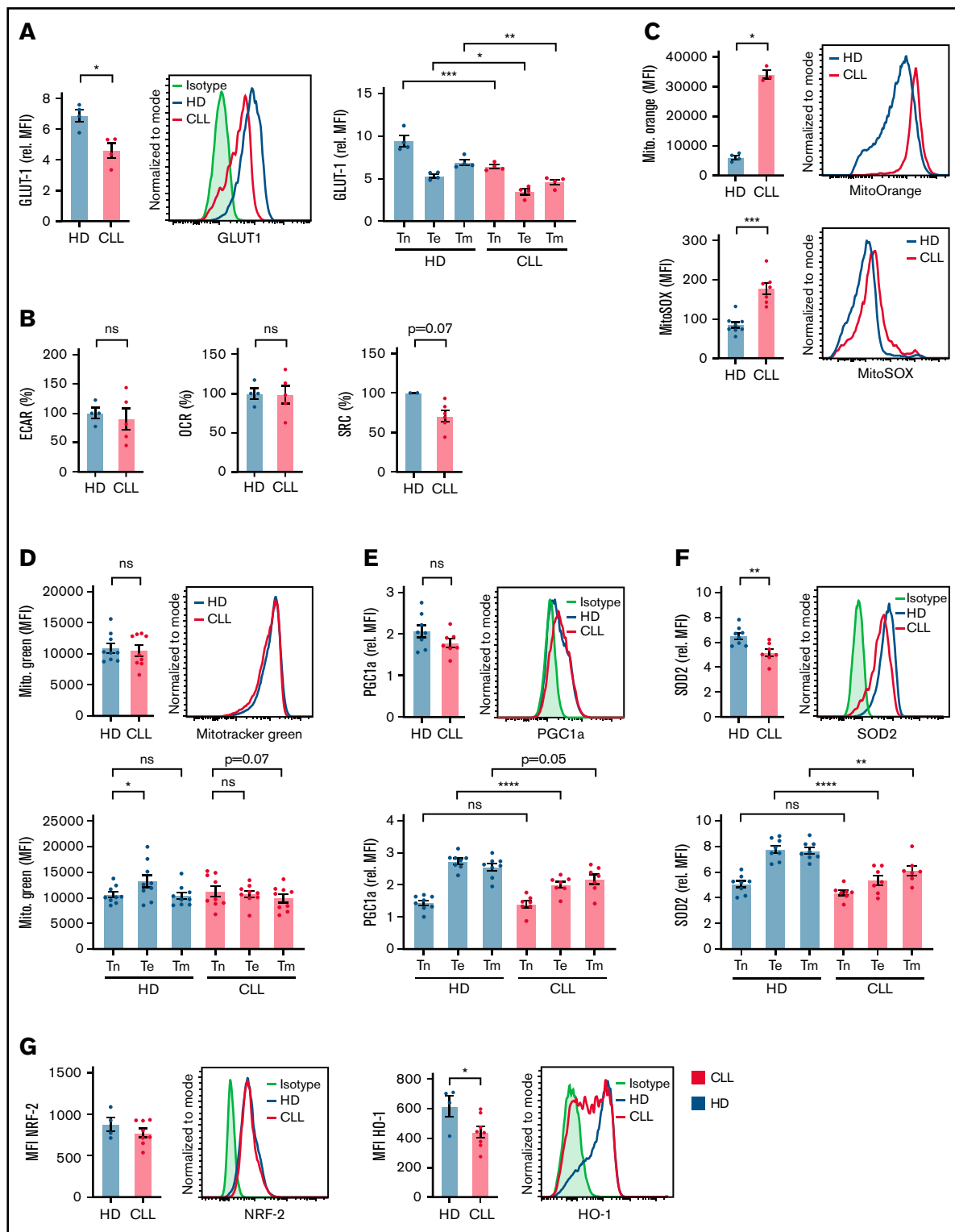


**Figure 2. Resting CLL T cells have an abnormal mitochondrial redox balance.** (A) PBMCs from patients with CLL and HDs were thawed, fixed or not, and stained, after which CD4 T cells were directly analyzed by flow cytometry for expression of total intracellular GLUT-1 storage in fixed CD4 T cells and subsets. Representative histogram of 1 HD (black) and 1 patient with CLL (red), as well as an isotype control (gray), is shown. (B) Analysis of extracellular flux (extracellular acidification rate [ECAR], OCR, and SRC) was performed by fluorescence-activated cell sorting of T cells first (purity >99%) and immediate measurement of the sorted cells for ECAR and OCR; the SRC could be derived from the OCR afterward. (C) Resting CD4 T cells were measured for mitochondrial potential and ROS production. Representative histogram of 1 HD (black), and 1 CLL patient (red) is shown, as well as an isotype control (gray). (D) Mitochondrial mass was analyzed in total resting CD4 T cells and subsets. A representative histogram of 1 HD (black) and 1 patient with CLL (red), as well as an isotype control (gray), is shown. PGC1a (E) and SOD2 (F) were measured in resting total CD4 T cells and subsets. Representative histogram of 1 HD (black) and 1 patient with CLL (red), as well as an isotype control (gray), is shown. (G) Expression of NRF-2 and HO-1 was measured in resting CD4 T cells. Representative histogram of 1 HD (black) and 1 patient with CLL (red), as well as an isotype control (gray), is shown. Each point represents a different HD or CLL patient. Data are presented as mean  $\pm$  standard error of the mean. \* $P < .05$ , \*\* $P < .005$ , \*\*\* $P < .001$ , \*\*\*\* $P < .0001$ . MFI, mean fluorescence intensity; ns, not significant; Te (effector), CD27<sup>-</sup>CD45RA<sup>+</sup>; Tm (memory), CD27<sup>+</sup>CD45RA<sup>-</sup>; Tn (naive), CD27<sup>+</sup>CD45RA<sup>+</sup>.

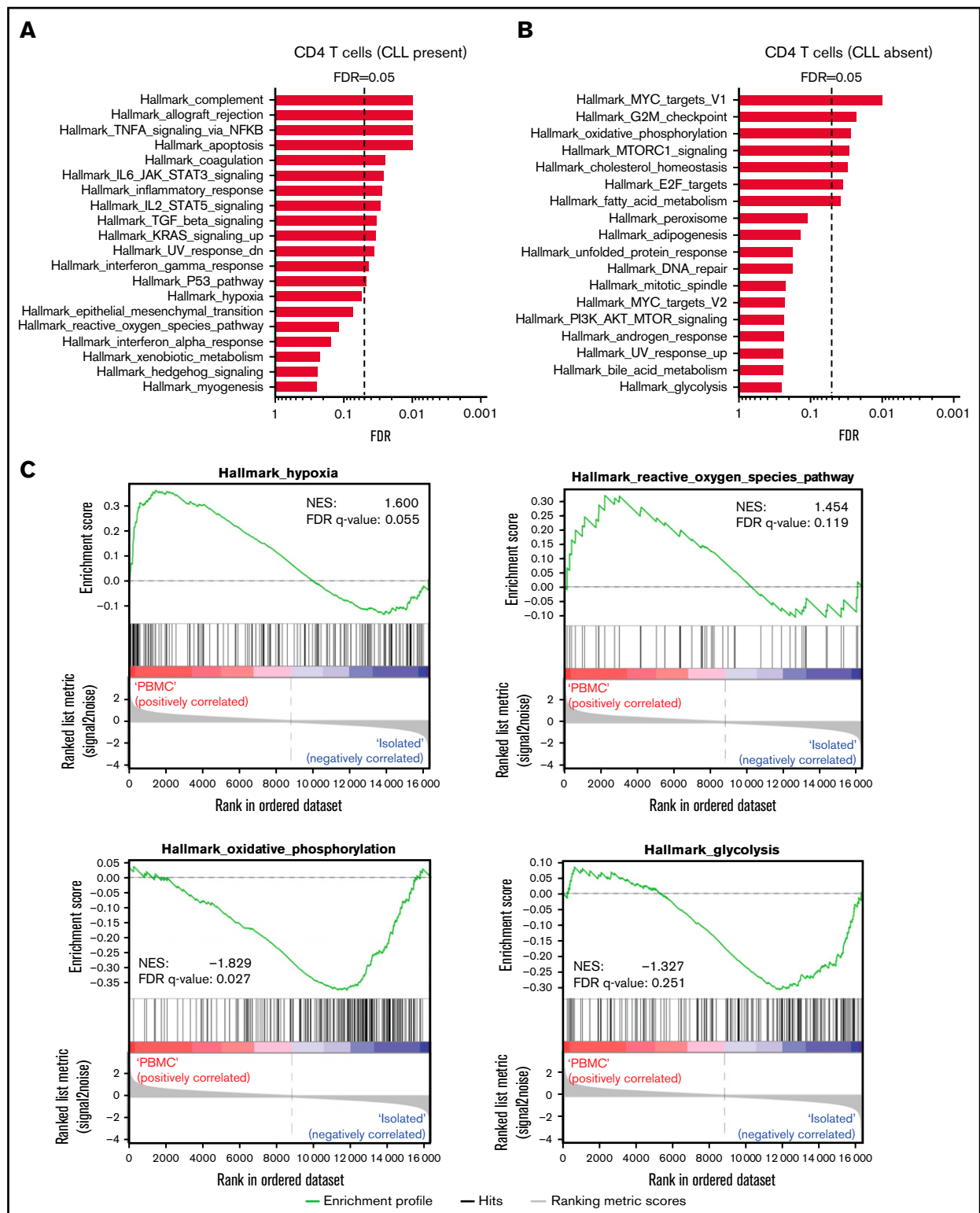


**Figure 3. ROS and hypoxia pathways are upregulated in activated CD4 T cells in presence of CLL, whereas OXPPOS and glycolysis are upregulated in absence of CLL.** PBMCs from patients with CLL and HDs were thawed, after which CD4 T cells from patients with CLL and HDs were cell sorted or not and subjected to CD3 plus CD28 stimulation for 2 days. GSEA against MSigDB Hallmark gene sets (h.all.v7.4) of 4 patients with CLL resulted in several pathways significantly upregulated in presence (A) and absence (B) of CLL cells. (C) Enrichment plots highlighting hypoxia, ROS, OXPPOS, and glycolysis pathways from analysis depicted in panels A and B. Genes are ranked by differential expression in PBMCs vs isolated cells on the x-axis; red indicates upregulation in PBMCs, and blue indicates upregulation in isolated cells. Curves (green) indicate cumulative enrichment quantified by enrichment score on the y-axis. Tick marks on the x-axis correspond to ranks of genes in the gene set. (D) Heat map showing differentially expressed genes in CLL-derived CD4 T cells stimulated with CD3 plus CD28 antibodies in presence or absence of CLL cells. Genes

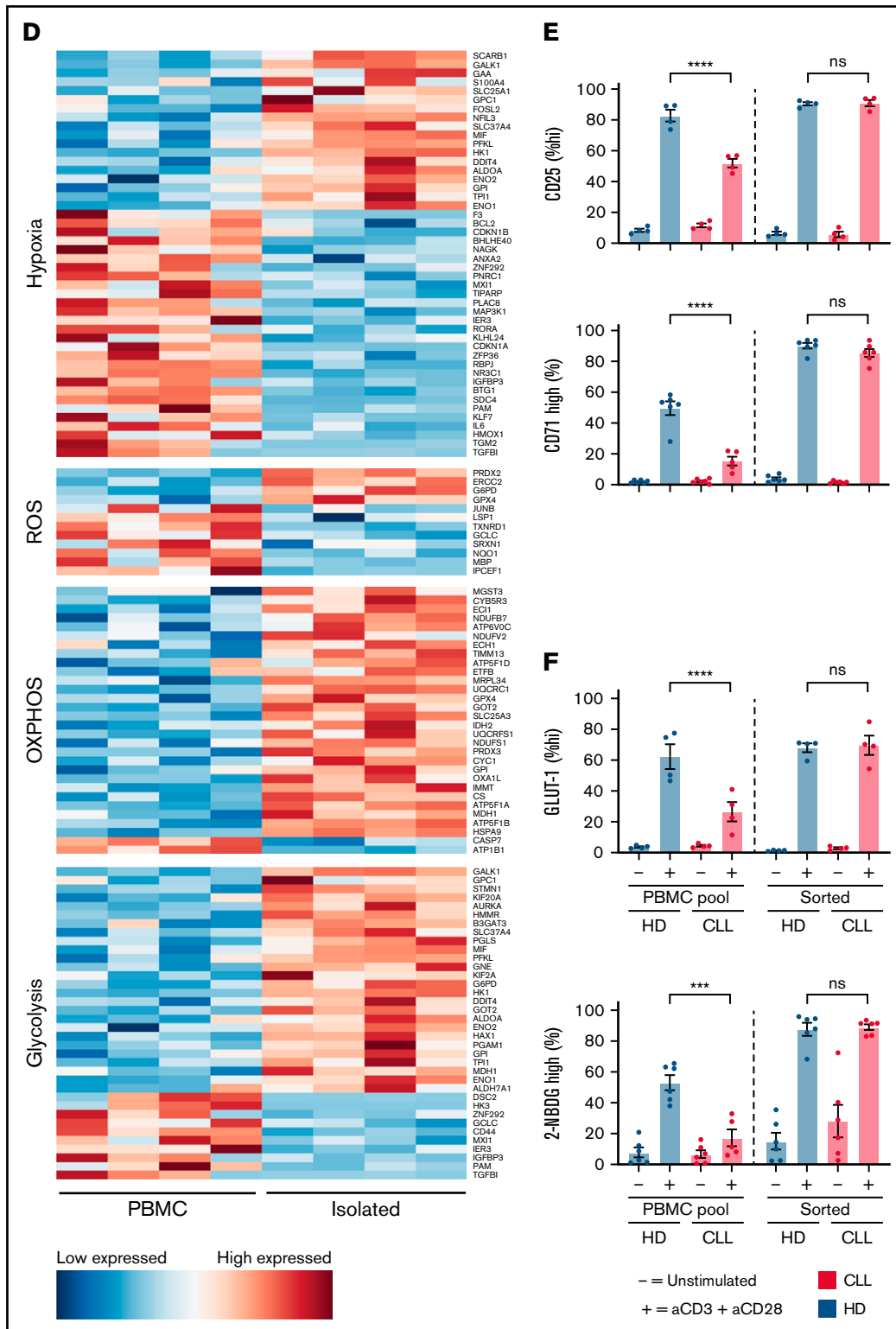


**Figure 3 (continued)** correspond to hypoxia, ROS, OXPHOS, and glycolysis pathways. Sorted or unsorted CD4 T cells from patients with CLL and HDs were stimulated with CD3 plus CD28 antibodies and analyzed for expression of CD25 and CD71 (E) and GLUT-1 expression and glucose uptake (2-NBDG) (F) using flow cytometry. (D-F) Each point represents a different HD or patient with CLL. Data are presented as mean  $\pm$  standard error of the mean.  $***P < .001$ ,  $****P < .0001$ . FDR, false-discovery rate; MFI, mean fluorescence intensity; ns, not significant.



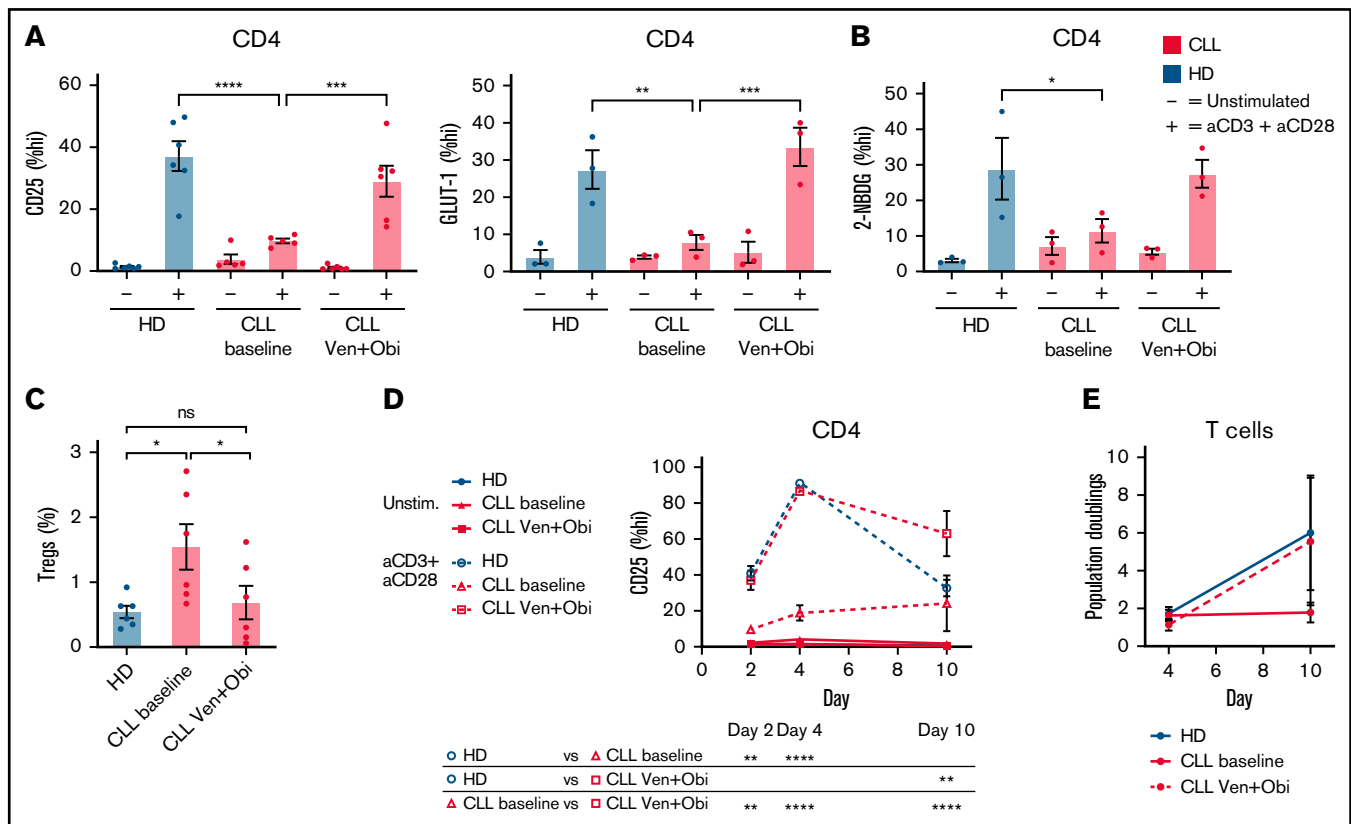


**Figure 4. Venetoclax treatment restores glycolytic switch and proliferation in CD4 T cells.** Patients with CLL who underwent 12 cycles of venetoclax had donated PBMCs before and after venetoclax plus obinutuzumab (Ven + Obi) treatment. (A) These PBMCs as well as PBMCs from HDs were thawed, after which we stimulated CD4 T cells and analyzed expression of CD25 and GLUT-1 before and after Ven + Obi treatment. (B) In this same experiment, glucose uptake (2-NBDG) was measured. (C) Presence of Tregs after Ven + Obi treatment. (D) Dynamic analysis of CD4 T-cell activation revealed a substantial improvement of CD4 T-cell activation after Ven + Obi treatment. (E) T cells from patients with CLL obtained before and after Ven + Obi treatment and from HDs were stimulated with CD3 plus CD28 antibodies and allowed to proliferate for 10 days. Proliferation was measured by flow cytometry using 123count eBeads. Each point represents a different HD or patient with CLL. Data are presented as mean  $\pm$  standard error of the mean. \* $P < .05$ , \*\* $P < .005$ , \*\*\* $P < .001$ , \*\*\*\* $P < .0001$ . ns, not significant.

*P* values of nonparametric distributions were calculated using the Mann-Whitney *U* test for unpaired data or Wilcoxon *t* test for paired data. A *t* test with Welch correction was used to test significance of differences between parametric and unpaired data sets, and an *F* test was used on data sets with unequal variance. Significance of parametric distributed paired data was calculated by using a paired *t* test. All statistical tests were calculated using Graphpad PRISM (version 9).

## Results

### Impaired glycolytic switch in CLL-derived CD4 T cells

PBMCs from patients with CLL and age-matched HDs were stimulated for 2 days and analyzed for T-cell activation, glycolytic switch, and mitochondrial health. CLL CD4 T cells expressed reduced levels of CD25, CD71, and 4-1BB upon CD3 or CD3 plus CD28 stimulation compared with HD cells (Figure 1A; supplemental Figure 1A). Prolonged stimulation revealed impaired proliferation of CLL-derived CD4 T cells (Figure 1B), as well as upregulation of PD-1 (Figure 1C; supplemental Figure 1A). We then analyzed expression of glucose transporter GLUT-1, because it is essential for CD4 T-cell function.<sup>26</sup> After 2 days of CD3 plus CD28

stimulation, a small population of CD4 T cells expressed GLUT-1 in samples from patients with CLL (Figure 1D; supplemental Figure 1A). Furthermore, GLUT-1 expression was lower in CLL T cells, even within activated T cells (gated on CD25-high CD4 T cells; supplemental Figure 1A), indicating impaired GLUT-1 trafficking to the cell surface, low GLUT-1 storages before T-cell activation, or reduced de novo GLUT-1 synthesis (Figure 1D). In accordance with low GLUT-1 expression, uptake of glucose was reduced in CLL CD4 T cells after both CD3 and CD3 plus CD28 stimulation compared with in HD cells (Figure 1E). Analysis of extracellular flux revealed a lower extracellular acidification rate (an indicator of glycolysis) but not OCR (indicator of OXPHOS) directly after CD3 plus CD28 stimulation of CLL CD4 T cells compared with HD cells (supplemental Figure 1B). Analysis of mitochondrial fitness revealed significantly elevated mitochondrial potential in CLL T cells, which was further enhanced after T-cell activation (Figure 1F; supplemental Figure 1C). Similarly, ROS produced by mitochondria were highly elevated in CLL T cells and also further increased after T-cell activation (Figure 1G; supplemental Figure 1C). Both elevated mitochondrial potential and ROS have been indicated as markers of exhausted T cells.<sup>27</sup> Mitochondrial biogenesis was not different between CLL and HD T cells (Figure 1H). These results show that

CD4 T cells have impaired T-cell activation, coinciding with low expression of GLUT-1 and glucose uptake and decreased mitochondrial fitness.

### Resting CLL CD4 T cells have abnormal mitochondrial redox balance

CLL CD4 T cells displayed impaired activation and glycolytic switch and impaired mitochondrial health after activation, which raised the question of whether differences could already be observed in the resting state before activation. We observed no difference in surface GLUT-1 expression in unstimulated CD4 T cells between samples from patients with CLL and those from HDs (Figure 1D). Analysis of total intracellular GLUT-1 stores revealed that CLL CD4 T cells had lower expression of GLUT-1 compared with HD cells (Figure 2A). This was not restricted to a specific T-cell subset (naïve, CD27<sup>+</sup>CD45<sup>+</sup>; effector, CD27<sup>-</sup>CD45<sup>+/+</sup>; memory, CD27<sup>+</sup>CD45<sup>-</sup>; supplemental Figure 2A), because GLUT-1 expression was decreased across naïve, effector, and memory subsets in CLL (Figure 2A). Analysis of extracellular flux showed no difference in basal extracellular acidification rate or basal OCR in resting T cells derived from patients with CLL and HDs, but a trend toward decreased SRC was observed, which reflects the capacity of a cell to deal with increased cellular bioenergetic demands such as T-cell activation<sup>28</sup> (Figure 2B; supplemental Figure 2B). Analysis of mitochondrial potential and ROS revealed substantial elevated levels of both mitochondrial potential and ROS in resting CD4 CLL T cells (Figure 2C). Mitochondrial mass was similar between HD and CLL cells, but analysis of mitochondrial mass of T-cell subsets revealed impaired mitochondrial biogenesis in antigen-experienced CD4 T cells (Figure 2D). These results prompted us to investigate drivers of mitochondrial biogenesis, as well as ROS scavengers responsible for mitigating ROS produced by mitochondria. Expression of PGC1a, the master regulator of mitochondrial biogenesis, was decreased in antigen-experienced CD4 T cells from patients with CLL (Figure 2E). In addition, ROS scavenger superoxide dismutase 2, which is regulated by PGC1a, was similarly reduced in expression (Figure 2F). In line with this, HO-1, a potent ROS scavenger, showed decreased expression in T cells in CLL (Figure 2G). Because NRF-2 was not different, downregulation of HO-1 likely occurs via an alternative route. Together, these results demonstrate that metabolic alterations are already visible in resting CD4 T cells. ROS balance in CLL CD4 T cells was particularly abrogated, indicating an impaired redox balance.

### ROS and hypoxia pathways are upregulated in activated CD4 T cells in presence of CLL, whereas OXPHOS and glycolysis are upregulated in absence of CLL

It has been demonstrated that CLL cells are able to directly impair T-cell function.<sup>29</sup> To assess whether CLL cells can induce transcriptional differences in metabolic genes, RNA sequencing was performed to define changes in metabolic pathways in an unbiased manner. For this experiment, CD4 T cells from patients with CLL were activated in the presence or absence of their autologous CLL cells; the paired design of this experiment eliminated possible confounding effects of T-cell subset composition. GSEA revealed differential regulation of numerous metabolic pathways (Figure 3A-B). For example, hypoxia and ROS were upregulated in the presence of CLL cells (Figure 3A,C), whereas OXPHOS and glycolysis were upregulated in the absence of

CLL cells (Figure 3B-C). A full list of significantly different genes within the 4 highlighted pathways is available in supplemental Table 4.

Key regulators of hypoxia such as HIF-1 $\alpha$  (*HIF1A*) and hypoxia-inducing factors (*EGLN1*, *EGLN2*, and *EGLN3*) were not significantly upregulated. However, hypoxia-associated genes such as *IGFBP3*, *BTG1*, *CDKN1A*, *CDKN1B*, and *ZFP36* were upregulated in the presence of CLL cells, indicating cell-cycle arrest and suppression of T-cell activation. Important ROS scavengers were downregulated in CD4 T cells activated in the presence of CLL cells: glutathione peroxidase 4 (*GPX4*) and peroxiredoxin 2 (*PRDX2*; Figure 3D). Conversely, NAD(P)H:quinone oxidoreductase 1 (*NQO1*), activity of which produces high levels of ROS, was upregulated in CD4 T cells activated in presence of CLL cells (Figure 3D). These results demonstrate that the redox balance in CD4 T cells in the presence of CLL cells is dysregulated.

In the absence of CLL cells, activated CD4 T cells significantly upregulated genes related to OXPHOS and glycolysis pathways, indicating that CD4 T-cell activation was normalized (Figure 3D). CD4 T cells activated in the absence of CLL cells upregulated genes involved in fatty acid  $\beta$ -oxidation (*ECI1* and *ECH1*) and genes related to complexes of the electron transport chain (complex 1, *NDUFB7* and *NDUFS1*; complex 3, *UQCRC1* and *CYC1*; complex 4, *COX6B1*; and complex 5, *ATP5F1D*, *ATP5F1B*, and *ATP5F1A*). Additionally, upregulation of ADP/ATP carrier genes (*SLC25A3* and *SLC25A5*), genes involved in the TCA cycle (*MDH2* and *CS*), and genes comprising the malate/aspartate shuttle (*MDH1* and *GOT2*) were also observed in CD4 T cells activated in the absence of CLL cells (Figure 3D). Whereas the glycolysis pathway as a whole was not significantly different between CD4 T cells stimulated in the presence and absence of CLL cells, a clear upregulation in genes involved in glycolysis was observed in CD4 T cells activated in the absence of CLL cells (*HK1*, *GPI*, *PFK-1*, *ALDOA*, *TPI1*, *PGAM1*, *ENO1*, and *ENO2*, the protein products of which all work together to transform glucose into pyruvate). In addition, the rate-limiting enzyme of the pentose phosphate pathway *G6PD* was also upregulated (Figure 3D). These results imply that the presence of CLL cells restricts CD4 T cells to upregulate OXPHOS, engage the pentose phosphate pathway, and efficiently switch to glycolysis after T-cell activation to ensure that their energy demands are met.

To confirm that upregulation of OXPHOS and glycolysis genes in CD4 T cells leads to restored activation, CD4 T cells were analyzed for expression of CD25 and CD71, which revealed complete reversal of impaired CD4 T-cell activation in the absence of CLL cells (Figure 3E). Concurrently, upregulation of GLUT-1 was observed (Figure 3F), which coincided with increased uptake of glucose in CD4 T cells in the absence of CLL cells (Figure 3F). Although PD-1 expression was not significantly decreased in sorted CLL-derived CD4 T cells after activation, a downward trend was observed, and PD-1 expression was reduced to levels similar to those in HD cells (supplemental Figure 3A). Collectively, these data demonstrate that metabolism of CD4 T cells is vastly influenced by the presence of CLL cells. Eliminating CLL cells before activation restored CD4 T-cell activation to levels observed in HD.



## Glycolytic switch and proliferation in CD4 T cells is restored after CLL depletion by venetoclax treatment

Because elimination of CLL cells restored T-cell function *in vitro*, we next wanted to identify whether metabolism and function of CD4 T cells would be restored after *in vivo* elimination of CLL after venetoclax treatment. Biobanked samples from the randomized phase 2 HOVON 139 trial<sup>30</sup> from baseline, before start of treatment, and after 1 year of treatment were used to study the impact of venetoclax plus obinutuzumab treatment on CD4 T-cell function and metabolism. In the intention-to-treat population, undetectable minimal residual disease level (defined by flow cytometry as  $<1$  CLL cell detected on 10 000 leukocytes [ $<10^{-4}$ ]) in PB and bone marrow was reached in 88% and 79% of patients, respectively, by the end of the planned 12 induction cycles.<sup>20</sup> Characteristics of 6 patients enrolled in the study are summarized in supplemental Table 3. For each patient, PBMCs were collected before therapy and at treatment cessation after 12 treatment cycles. T cells from both these samples were then stimulated and analyzed; CD4 T cells isolated before treatment showed impaired T-cell activation, whereas CD4 T cells isolated after venetoclax plus obinutuzumab treatment were activated and expressed CD25 and GLUT-1 at similar levels compared with HD CD4 T cells (Figure 4A). In accordance with upregulated GLUT-1, glucose uptake as shown by increased levels of 2-NBDG was also normalized to HD levels after venetoclax plus obinutuzumab treatment (Figure 4B). Presence of Tregs has often been described as a marker of clinical significance in CLL because of their immunosuppressive effect, increasing with disease progression.<sup>31–33</sup> The proportion of Tregs was reduced after venetoclax plus obinutuzumab treatment (Figure 4C; supplemental Figure 3B). In addition, dynamic analysis of CD4 T-cell activation of both CD4 T cells isolated before therapy and after 12 cycles demonstrated enhanced expression of CD25 in venetoclax plus obinutuzumab-treated patients over time, similar to levels in HDs (Figure 4D). Moreover, venetoclax plus obinutuzumab treatment enhanced proliferation of T cells from patients with CLL compared with untreated matched baseline samples, similar to age-matched healthy controls (Figure 4E). Thus, T cells derived from patients with CLL showed a high degree of plasticity after elimination of CLL cells by treatment with venetoclax long term, and when activating posttreatment T cells *in vitro*, activation and proliferation was fully restored. In addition, venetoclax plus obinutuzumab treatment normalized Treg proportions in CLL.

## Discussion

Our study describes impaired activation of CLL-derived CD4 T cells, which coincided with decreased mitochondrial fitness and failure to switch to glycolysis, an essential feature for CD4 T-cell effector function and ability to proliferate.<sup>26</sup> In addition, recovery of T-cell function was possible by either *in vitro* depletion of CLL cells before stimulation or *in vivo* depletion by treatment, together indicating that CLL CD4 T cells demonstrate plasticity that can be exploited for autologous T cell–based treatment regimes.

Previous studies have demonstrated that CLL cells impose functional defects on T cells, a phenotype that could be replicated in HD T cells.<sup>8,29</sup> Because T-cell metabolism drives T-cell fate and function,<sup>9</sup> we hypothesized that CLL cells interfere with CD4 T cells to induce an immunosuppressive environment. We show that elimination of CLL

cells not only improved CD4 T-cell activation but also resulted in transcriptional changes in ROS and hypoxia pathways toward OXPHOS and glycolysis. This implies that CLL cells actively suppress CD4 T-cell metabolism. An important feature of T-cell activation is expression of GLUT-1 to enable glucose uptake, which is essential for CD4 T-cell effector function.<sup>9,26,34</sup> This is further reflected in murine GLUT-1 knockout models. Resting GLUT-1 knockout CD4 T cells could survive but had impaired proliferation and low expression of CD71 after activation,<sup>26</sup> which is in line with our results. In fact, low intracellular GLUT-1 in CLL-derived T cells may have a causal role in dysfunction, because it is essential to increase the glycolytic flux required for T-cell effector function and creation of cellular biomass required for cellular division.<sup>34</sup> In addition, our results show that mitochondrial potential and ROS were elevated in resting T cells in CLL, indicative of cellular stress, reduced mitochondrial fitness, and diminished effector function.<sup>27</sup> Indeed, adoptive transfer of murine glycoprotein 100 peptide-specific T cells sorted based on high or low mitochondrial potential showed increased persistence and proliferative capacity of T cells, which were sorted based on low mitochondrial potential after a recall response with glycoprotein 100 vaccinia virus.<sup>27</sup> Furthermore, T cells with high mitochondrial potential displayed an effector phenotype with low proliferative potential and high levels of ROS coinciding with lower expression of antioxidant genes.<sup>27</sup> These and our results confirm that T-cell dysfunction is characterized by deteriorated mitochondrial fitness, which coincides with a failure to switch to glycolysis. We previously found indications of a soluble factor responsible for CLL-mediated CD8 T-cell dysfunction.<sup>7</sup> Another explanation might be that T-cell function is actively repressed by expression of CD24 and CD52 on CLL cells suppressing T-cell activation via Siglec-10.<sup>35</sup> However, more investigation on this subject is required to define the exact mechanism of T-cell dysfunction in T cells in CLL and how it subsequently affects T-cell metabolism.

Currently available targeted therapies have the capacity to efficiently eliminate CLL cells in patients, especially in the early treatment period when resistance hardly occurs.<sup>36,37</sup> Our laboratory previously demonstrated reconstitution of immune cell composition in patients with CLL after venetoclax plus obinutuzumab treatment.<sup>15</sup> Treatment with venetoclax plus obinutuzumab resulted in reduction of protumoral CD4 T-cell subsets, such as T follicular helper cells and Tregs, and resulted in improvement of T-cell effector function.<sup>15</sup> Direct effects of venetoclax on metabolism of cancer cells have been observed as well, including inhibition of mitochondrial respiration.<sup>38,39</sup> Our current results demonstrate that treatment with venetoclax does not necessarily result in defective T-cell responses, similar to previous observations.<sup>15,40</sup> In accordance with this, venetoclax treatment combined with PD-1–blocking antibodies resulted in superior antitumor efficacy over treatment with PD-1 antibodies alone in a mouse colon adenocarcinoma model, indicating that venetoclax does not antagonize T-cell function.<sup>40</sup> Whether venetoclax also inhibits mitochondrial respiration in CD4 T cells, as has been described for cancer cells,<sup>38,39</sup> remains to be determined. If so, other effects of venetoclax (eg, CLL elimination) or the addition of other treatment regimens (obinutuzumab or PD-1–blocking antibodies) could overrule this potential negative effect. Our observations indicate that T-cell function is indirectly improved by venetoclax as a result of elimination of CLL cells. Therefore, we hypothesize that similar effects may be achieved by treatment regimens that result in

the elimination of CLL cells. Indeed, treatment of CLL with both venetoclax and ibrutinib resulted in overall improvements in the immune cell compartment.<sup>15</sup> Our results incentivize investigation of whether the efficacy of alternative autologous-based therapies, such as chimeric antigen receptor (CAR) T-cell therapy, can be similarly improved in vivo after venetoclax treatment or by adapting the CAR T cells to restore redox balance. This has yet to be described in CLL but could possibly be achieved by designing a CAR that allows expression of the CAR itself and expression of a gene essential for achieving redox balance in tandem. Obinutuzumab has been reported to moderately deplete CD4 and CD8 T cells in patients with CLL. However, our results show that this does not affect T-cell function.<sup>41</sup> In conclusion, our results demonstrate that CLL cells impose metabolic alterations on CD4 T cells. Because T-cell metabolism is intricately linked to function and development, the current hypothesis is that CD4 T-cell fate is directly altered by CLL cells through metabolism. Future experimental models will need to define how to pharmacologically intervene in this process. This may lead to improvements in future T cell-based therapies.

## Acknowledgments

The authors thank the patients and healthy donors for their blood donations.

## References

1. Hallek M, Cheson BD, Catovsky D, et al. iwCLL guidelines for diagnosis, indications for treatment, response assessment, and supportive management of CLL. *Blood*. 2018;131(25):2745-2760.
2. Zhang S, Kipps TJ. The pathogenesis of chronic lymphocytic leukemia. *Annu Rev Pathol*. 2014;9:103-118.
3. Cutucache CE. Tumor-induced host immunosuppression: special focus on CLL. *Int Immunopharmacol*. 2013;17(1):35-41.
4. DiLillo DJ, Weinberg JB, Yoshizaki A, et al. Chronic lymphocytic leukemia and regulatory B cells share IL-10 competence and immunosuppressive function. *Leukemia*. 2013;27(1):170-182.
5. Riches JC, Davies JK, McClanahan F, et al. T cells from CLL patients exhibit features of T-cell exhaustion but retain capacity for cytokine production. *Blood*. 2013;121(9):1612-1621.
6. te Raa GD, Pascutti MF, García-Vallejo JJ, et al. CMV-specific CD8<sup>+</sup> T-cell function is not impaired in chronic lymphocytic leukemia. *Blood*. 2014;123(5):717-724.
7. van Bruggen JAC, Martens AWJ, Fraietta JA, et al. Chronic lymphocytic leukemia cells impair mitochondrial fitness in CD8<sup>+</sup> T cells and impede CAR T-cell efficacy. *Blood*. 2019;134(1):44-58.
8. Ramsay AG, Johnson AJ, Lee AM, et al. Chronic lymphocytic leukemia T cells show impaired immunological synapse formation that can be reversed with an immunomodulating drug. *J Clin Invest*. 2008;118(7):2427-2437.
9. Buck MD, O'Sullivan D, Pearce EL. T cell metabolism drives immunity. *J Exp Med*. 2015;212(9):1345-1360.
10. Chang CH, Qiu J, O'Sullivan D, et al. Metabolic competition in the tumor microenvironment is a driver of cancer progression. *Cell*. 2015;162(6):1229-1241.
11. Siska PJ, van der Windt GJ, Kishton RJ, et al. Suppression of Glut1 and glucose metabolism by decreased Akt/mTORC1 signaling drives T cell impairment in B cell leukemia. *J Immunol*. 2016;197(6):2532-2540.
12. van Bruggen JAC, Martens AWJ, Tonino SH, Kater AP. Overcoming the hurdles of autologous T-cell-based therapies in B-cell non-Hodgkin lymphoma [published correction appears in *Cancers (Basel)*. 2021;13(19):4738]. *Cancers (Basel)*. 2020;12(12):3837.
13. Roessner PM, Seiffert M. T-cells in chronic lymphocytic leukemia: guardians or drivers of disease? [published correction appears in *Leukemia*. 2021;35(12):3634]. *Leukemia*. 2020;34(8):2012-2024.
14. Peters FS, Strefford JC, Eldering E, Kater AP. T-cell dysfunction in chronic lymphocytic leukemia from an epigenetic perspective. *Haematologica*. 2021;106(5):1234-1243.
15. de Weerd I, Hofland T, de Boer R, et al. Distinct immune composition in lymph node and peripheral blood of CLL patients is reshaped during venetoclax treatment. *Blood Adv*. 2019;3(17):2642-2652.
16. Yin Q, Sivina M, Robins H, et al. Ibrutinib therapy increases T cell repertoire diversity in patients with chronic lymphocytic leukemia. *J Immunol*. 2017;198(4):1740-1747.

This work was supported by Dutch Research Council Health Research and Development Vidi Talent Programme 917 15 33 (A.P.K.) and European Research Council Bootcamp grant 864815 (A.P.K.).

## Authorship

Contribution: J.A.C.v.B., G.J.W.v.d.W., F.S.P., and A.P.K. designed the research; M.H. collected patient samples; J.A.C.v.B. and G.J.W.v.d.W. performed the research and analyzed the data; J.A.C.v.B., G.J.W.v.d.W., J.D., F.S.P., and A.P.K. wrote the paper; and M.H. corrected the article.

Conflict-of-interest disclosure: A.P.K. receives research funding from AbbVie for the clinical trials described in this article. The remaining authors declare no competing financial interests.

ORCID profiles: J.A.C.v.B., 0000-0002-0636-6754; A.P.K., 0000-0003-3190-1891; F.S.P., 0000-0002-0509-315X.

Correspondence: Arnon P. Kater, Department of Hematology, Amsterdam UMC, University of Amsterdam, Meibergdreef 9, 1105 AZ Amsterdam, The Netherlands; e-mail: a.p.kater@amsterdamumc.nl.

17. Long M, Beckwith K, Do P, et al. Ibrutinib treatment improves T cell number and function in CLL patients. *J Clin Invest*. 2017;127(8):3052-3064.
18. Kater AP, Seymour JF, Hillmen P, et al. Fixed duration of venetoclax-rituximab in relapsed/refractory chronic lymphocytic leukemia eradicates minimal residual disease and prolongs survival: post-treatment follow-up of the MURANO phase III study. *J Clin Oncol*. 2019;37(4):269-277.
19. Hoy SM. Obinutuzumab: a review of its use in patients with chronic lymphocytic leukaemia. *Drugs*. 2015;75(3):285-296.
20. Kersting S, Dubois J, Nasserinejad K, et al; HOVON CLL study group. Venetoclax consolidation after fixed-duration venetoclax plus obinutuzumab for previously untreated chronic lymphocytic leukaemia (HOVON 139/GiVe): primary endpoint analysis of a multicentre, open-label, randomised, parallel-group, phase 2 trial. *Lancet Haematol*. 2022;9(3):e190-e199.
21. Mackus WJ, Frakking FN, Grummels A, et al. Expansion of CMV-specific CD8+CD45RA+CD27- T cells in B-cell chronic lymphocytic leukemia. *Blood*. 2003;102(3):1057-1063.
22. van der Windt GJW, Chang CH, Pearce EL. Measuring bioenergetics in T cells using a Seahorse Extracellular Flux Analyzer. *Curr Protoc Immunol*. 2016;113:3.16B.1-3.16B.14.
23. Dobin A, Davis CA, Schlesinger F, et al. STAR: ultrafast universal RNA-seq aligner. *Bioinformatics*. 2013;29(1):15-21.
24. Li B, Dewey CN. RSEM: accurate transcript quantification from RNA-Seq data with or without a reference genome. *BMC Bioinformatics*. 2011;12:323.
25. Love MI, Huber W, Anders S. Moderated estimation of fold change and dispersion for RNA-seq data with DESeq2. *Genome Biol*. 2014;15(12):550.
26. Macintyre AN, Gerriets VA, Nichols AG, et al. The glucose transporter Glut1 is selectively essential for CD4 T cell activation and effector function. *Cell Metab*. 2014;20(1):61-72.
27. Sukumar M, Liu J, Mehta GU, et al. Mitochondrial membrane potential identifies cells with enhanced stemness for cellular therapy. *Cell Metab*. 2016;23(1):63-76.
28. van der Windt GJ, Everts B, Chang CH, et al. Mitochondrial respiratory capacity is a critical regulator of CD8+ T cell memory development. *Immunity*. 2012;36(1):68-78.
29. Ramsay AG, Clear AJ, Fatah R, Gribben JG. Multiple inhibitory ligands induce impaired T-cell immunologic synapse function in chronic lymphocytic leukemia that can be blocked with lenalidomide: establishing a reversible immune evasion mechanism in human cancer. *Blood*. 2012;120(7):1412-1421.
30. Kater AP, Kersting S, van Norden Y, et al; HOVON CLL study group. Obinutuzumab pretreatment abrogates tumor lysis risk while maintaining undetectable MRD for venetoclax + obinutuzumab in CLL. *Blood Adv*. 2018;2(24):3566-3571.
31. Giannopoulos K, Schmitt M, Kowal M, et al. Characterization of regulatory T cells in patients with B-cell chronic lymphocytic leukemia. *Oncol Rep*. 2008;20(3):677-682.
32. Jadidi-Niaragh F, Yousefi M, Memarian A, et al. Increased frequency of CD8+ and CD4+ regulatory T cells in chronic lymphocytic leukemia: association with disease progression. *Cancer Invest*. 2013;31(2):121-131.
33. Lad DP, Varma S, Varma N, Sachdeva MU, Bose P, Malhotra P. Regulatory T-cells in B-cell chronic lymphocytic leukemia: their role in disease progression and autoimmune cytopenias. *Leuk Lymphoma*. 2013;54(5):1012-1019.
34. Palmer CS, Ostrowski M, Balderson B, Christian N, Crowe SM. Glucose metabolism regulates T cell activation, differentiation, and functions. *Front Immunol*. 2015;6:1.
35. Van Bruggen JAC, Peters F, Cretenet G, Melenhorst JJ, Eldering E, Kater AP. Chronic lymphocytic leukemia actively induces T-cell dysfunction by contact-dependent signaling via CD24 and CD52. *Blood*. 2021;138(Supplement 1):3714.
36. Herling CD, Cymbalista F, Groß-Ophoff-Müller C, et al. Early treatment with FCR versus watch and wait in patients with stage Binet A high-risk chronic lymphocytic leukemia (CLL): a randomized phase 3 trial. *Leukemia*. 2020;34(8):2038-2050.
37. Shustik C, Mick R, Silver R, Sawitsky A, Rai K, Shapiro L. Treatment of early chronic lymphocytic leukemia: intermittent chlorambucil versus observation. *Hematol Oncol*. 1988;6(1):7-12.
38. Roca-Portoles A, Rodriguez-Blanco G, Sumpton D, et al. Venetoclax causes metabolic reprogramming independent of BCL-2 inhibition. *Cell Death Dis*. 2020;11(8):616.
39. Pollyea DA, Stevens BM, Jones CL, et al. Venetoclax with azacitidine disrupts energy metabolism and targets leukemia stem cells in patients with acute myeloid leukemia. *Nat Med*. 2018;24(12):1859-1866.
40. Kohlhapp FJ, Haribhai D, Mathew R, et al. Venetoclax increases intratumoral effector T cells and antitumor efficacy in combination with immune checkpoint blockade. *Cancer Discov*. 2021;11(1):68-79.
41. García-Muñoz R, Aguinaga L, Feliu J, et al. Obinutuzumab induces depletion of NK cells in patients with chronic lymphocytic leukemia. *Immunotherapy*. 2018;10(6):491-499.